Received: 17 December 2020 | Revised: 25 March 2021 | Accepted: 12 April 2021

DOI: 10.1096/fj.202002738R

RESEARCH ARTICLE

THE FASEB JOURNAL

Circular RNA circUbe2k promotes hepatic fibrosis via sponging miR-149-5p/TGF-β2 axis

Sai Zhu[1,2,3] | **Xin Chen**[1,2,3] | **Jia-Nan Wang**[1,2,3] | **Jin-Jin Xu**[1,2,3] | **Ao Wang**[1,2,3] | **Juan-Juan Li**[1,2,3] | **Sha Wu**[1,2,3] | **Yuan-Yuan Wu**[1,2,3] | **Xiao-Feng Li**[1,2] | **Cheng Huang**[1,2,3] | **Jun Li**[1,2,3]

[1]Inflammation and Immune Mediated Diseases Laboratory of Anhui Province, Hefei, China

[2]Anhui Institute of Innovative Drugs, Hefei, China

[3]School of Pharmacy, Anhui Medical University, Hefei, China

Correspondence
Cheng Huang and Jun Li, School of Pharmacy, Anhui Medical University Hefei 230032, Anhui, China.
Email: huangcheng@ahmu.edu.cn (C. H.) and lj@ahum.edu.cn (J. L.)

Funding information
National Science Foundation of China, Grant/Award Number: 81770609, 81970534 and U19A2001; Anhui Medical University of Science and Technology, Grant/Award Number: 1704a0802161

Abstract

Abundant regulatory genes and complex circuits involving non-coding RNAs (ncRNAs) monitor the formation and development of hepatic fibrosis (HF). Circular RNAs (circRNAs) are a class of RNAs generated from protein coding genes by back-splicing, playing crucial roles in various pathological processes, including HF. However, little is known about mechanisms of action of circRNAs, let alone in HF. In this study, we found circUbe2k enhanced in CCl_4-induced HF mice and LX-2 cells stimulated with TGF-β1, regulating the development of HF. Restraining the expression of circUbe2k inhibited α-SMA and Col1α1 expression in CCl_4-induced HF mice and in LX-2 cells stimulated with TGF-β1. Furthermore, inhibiting circUbe2k expression reduced hepatic stellate cells (HSCs) activation and proliferation in vivo and in vitro. Mechanistically, we demonstrated a direct interaction between circUbe2k and miR-149-5p, which results in the modulation of TGF-β2 expressions. Together, circUbe2k may act as a "catalyst" of HSCs activation and HF through the circUbe2k/miR-149-5p/TGF-β2 axis. Our results provide unprecedented evidence for a significant role for circUbe2k to serve as a potential biomarker for HF therapy.

KEYWORDS

circUbe2k, circular RNA, hepatic fibrosis, miR-149-5p, TGF-β2

1 | INTRODUCTION

As the result of chronic liver disease, hepatic fibrosis (HF), a wound-healing response to repeated liver injury, which is characterized by excessive deposition of extracellular matrixes (ECM).[1-3] Persistent HF may evolve into cirrhosis, liver failure, or even liver cancer.[4] Early HF may be halted and even reversed after withdrawal of the underlying cause of disease by intervention.[5] Moreover, it has been widely confirmed that the activation and proliferation of hepatic stellate

Abbreviations: CAV1, caveolin 1; CDC9, coiled-coil domain containing 9; Col1α1, collagen Type I Alpha 1; FBXW4, F box and WD 40 domain containing protein 4; FBXW7, F box and WD 40 domain containing protein 7; PLK1, polo-like kinase 1; TGF-β1, transforming growth factor-β1; TGF-β2, transforming growth factor-β2; TIMP-1, TIMP metallopeptidase inhibitor 1; Ube2k, ubiquitin conjugating enzyme E2 K; α-SMA, α-smooth muscle actin.

Sai Zhu, Xin Chen, and Jia-Nan Wang contributed equally to this work.

cells (HSCs) are the major producers of ECM and serve as the hallmark of HF.[6] Activation of HSCs is a vital process in ECM deposition in damaged liver,[7] during which many pro-fibrogenic growth factors and cytokines initiate myofibroblastic differentiation, such as (TGF-β1).[8]

Mammalian cells conceal thousands of RNA molecules that do not contain coding proteins, but play a vital role in regulating physiological processes, the epigenetic regulation of proteins expression by the widespread noncoding RNAs (ncRNAs) including microRNA (miRNA), long ncRNA (lncRNA), and circularRNA (circRNA).[9,10] Although discovery of circRNAs was exposed more than 20 years ago, for many years they were thought to be functionless byproducts of mRNA splicing.[11,12] Recently, many researches reveal that circRNAs play a critical role in the diagnosis and prognosis of various diseases.[13,14] It is reported that circRNA is characterized by covalently closed loop structures neither 5′ to 3′ polarity nor a polyadenylated tail,[15] is single-stranded transcripts generated via back-splicing.[16] According to research, the biological function of circRNAs is separated into the following categories: act as a miRNA sponge,[17] a RNA-binding proteins and protein decoys,[18] a regulators of transcription.[19,20] Interestingly, miRNA sponging, which is circRNA act as competitive endogenous RNA (ceRNA) to keep miRNA away from their target gene, is the most commonly reported role of circRNAs.[21] For example, circular RNA circCCDC9 can act as a miR-6792-3p sponge to suppress the progression of gastric cancer through regulating CAV1 expression.[22] In recent years, our group had committed ourselves to exploring the relationship between the ncRNAs and HF for a long time.[23] We found that miRNA-203 play a part in liver injury and inflammation,[24] while miRNA-200a acts as a regulator in the initiation of HF.[25] Furthermore, we have explored the regulatory mechanism of circRNA in the formation and reversal of HF, like circular RNA circFBXW4 can target the miR-18b-3p/FBXW7 axis to suppress HF.[26] Furthermore, our group also has explored on the mechanism of generation and development of HF.[27] We found that PLK1 downregulation promotes HSCs apoptosis and reduces HF through Wnt/β-catenin signaling pathway in vivo and in vitro.[28] Even so, it has been shown that multiply circRNAs dysregulated in HF,[29] expression situation, biological function, and molecular mechanism of circRNAs in HF, especially HSCs, remain largely unknown and need further investigation. It is of great significance to explore the relationship between abnormal expression of circRNAs in HSCs and the treatment of HF.

In this study, we analyzed the expression situation of circRNAs, miRNAs and mRNAs in CCl_4-induced HF mice, attempting to explore the probable influence related to HF progression and pathological stages. We found a novel circRNA circUbe2k (mmu_circ_0001350), which comes from Ube2k gene locus via back-splicing. Interestingly, circUbe2k significantly increased in the liver fibrogenesis stage. Functionally, depressing the expression of circUbe2k inhibited the activation and proliferation of HSCs, reduced the collagen and ECM deposition, setting out an anti-fibrotic effect of circUbe2k in HF. Mechanistically, we found that circUbe2k binds to miR-149-5p, as a miRNA sponge, regulating the expression of TGF-β2, indicating that the circUbe2k/miR-149-5p/TGF-β2 axis plays crucial roles in HSCs activation and HF. Therefore, our study shows that circUbe2k may consider as a promising biomarker for HF therapy and may consider as a new strategy for the prevention of HF. To our knowledge, this is the first report investigates the expression profile, regulatory function and mechanism of circUbe2k in HF.

2 | MATERIALS AND METHODS

2.1 | Animals and treatments

Littermate male C57BL/6J mice (8 week of age) were purchased from Animal Experiment Center of Anhui Medical University. In this study, all the experiments of animal were reviewed and approved by the Animal Experimentation Ethics Committee of Anhui Medical University. C57BL/6J mice intraperitoneally injected two times a week (10% solution of CCl_4 in olive oil, 0.001 mL/g) for 6 weeks. Vehicle control mice received the same volume of olive oil only. Mice euthanized three days after the final injection.

2.2 | Adeno-associated virus (AAV) infection

Purified adeno-associated viral vector serotype 8 (AAV8) encoding circUbe2k and vector were structured by Hanheng Biotechnology (Shanghai, China). C57BL/6J mice were injected into the tail vein with AAV8 encoding circUbe2k and vector at 1×10^{12} vg/mL. One week later, HF model established for six weeks after AAV8 administration. The transfection efficiency measured by real-time PCR analysis.

2.3 | Histology and immunohistochemistry

4% Paraformaldehyde-fixed and paraffin-embedded liver tissues were sectioned at 4 μm thickness for hematoxylin and eosin (HE) and Sirius red staining, and immunohistochemical staining of α-SMA (1:400, Abcam, USA) and TGF-B2 (1:500, Bioss, China) to examine liver pathology.[30] These sections scanned by a digital slide scanner (Pannoramic MIDI, 3DHISTECH, Hungary).

2.4 | Serum biochemical value analysis

Serum was collected by centrifugation from the whole blood sample with 1000 *g* for 30 minutes at room temperature. The index of serum ALT and AST measured by using ALT and AST Assay Kit (Jiancheng Bioengineering Institute, Nanjing, China) according to the manufacturer's instructions.

2.5 | DNA sequencing

The RNA was reverse-transcribed into cDNA using PrimeScript RT Master Mix (Takara, Japan). Polymerase chain reaction (PCR) was performed using 2×Taq Master Mix (Takara, Japan) from the manufacturer's protocol. PCR products were identified by DNA sequencer (ABI3730XL, USA).

2.6 | Western blot analysis

The whole-protein lysates were prepared in RIPA buffer (Beyotime, China) separated by 10% SDS-PAGE electrophoretically and transferred onto PVDF membrane (Millipore, USA). After blocking with 5% skim milk for 1 hour at room temperature, the membranes were incubated with primary antibodies over night for 4°C. In this study, Antibodies adopted in western blotting: β-actin (1:500, Bioss, China), col1α1 (1:500, Bioss, China), α-SMA (1:500, Bioss, China), TGF-β2 (1:500, Bioss, China). Membranes were followed by incubations with the HRP-coupled secondary antibodies (1:10 000, ZSGB-Bio, China) for 6 minutes at room temperature. The protein signals were detected using chemiluminescent (ECL) system (Bio-Rad, USA) and were analyzed using IMAGE J software (National Institutes of Health, USA).

2.7 | Real-time PCR analysis

The total RNA were collected from liver tissues or LX-2 cells using TRIzol reagent (Invitrogen, USA) according to the manufacturer's protocols. Quantitative detection performed using a Spectrophotometer NanoDrop 2000 (Thermo Scientific, USA) and cDNA synthesized using PrimeScriptRT Master Mix (Takara, Japan), paired samples adjusted to the similar concentration for used. Divergent primers designed to measure the relative expression levels of circRNAs. qRT-PCR assay was performed using the CFX96 RT-PCR system (Bio-Rad, CA) with SYBR Premix Ex Taq II (Takara, Japan). MiRNA levels were measured using the Bulge-Loop miRNA qPCR Primer Set (RiboBio) according to the manufacturer's instructions. The expression of GAPDH was served as to internal control the data and the sequences of primers were listed in Table S1.

2.8 | Cell culture

The LX-2 cells (human immortalized HSC line) were cultured with DMEM (Gibco, USA) supplemented with 10% fetal bovine serum (Gibco, USA), 100 U/mL penicillin, and 100 mg/mL streptomycin, incubated with 5% CO_2 incubator at 37°C.

2.9 | Transfection with siRNA-circUbe2k in vitro

Small interfering RNAs (siRNAs) of circUnbe2k structured to target the junction site of circUbe2k. The sequence of siRNA listed in Table S2. The LX-2 cells were transfected with siRNA-circUbe2k (HanHeng, China) by Lipofectamine 2000 (Invitrogen, USA) from the manufacturer's protocol. After transfected for 6 hours, the culture medium replaced with fresh medium for an additional 48-hour incubation. The transfection efficiency measured by real-time PCR analysis.

2.10 | CCK-8 analysis

The proliferation of LX-2 cells was measured by a cell counting kit-8 assay. Transfected cells were collected and added to 96-well plates, incubated at 37°C overnight. CCK-8 solution (10 μL) added to each well for 2 hours, the absorbance value of each well at 450 nm was measured using the microplate reader (Bio-Tek EL, USA).

2.11 | Cell proliferation assay (5-Ethynyl-2′-deoxyuridine assay)

The EdU assay was performed using an EdU Cell Proliferation Kit (Beyotime, China). Briefly, transfected LX-2 cells seeded in a six-well plate and incubated for 24 hours. Then incubation with 10 μM EdU for 2 hours. Next, cells fixed with 4% paraformaldehyde at RT for 15 minutes, followed by 0.3% Triton X-100 to permeabilize cell. The cell nucleic acids were stained with Hoechst33342. Images were detected using an inverted fluorescence microscope (OLYMPUS IX83, Japan) and the percentage of EdU-positive cells was calculated.

2.12 | Cell cycle analysis

The amount of DNA present in the LX-2 cells was assessed by cell cycle analysis kit (Beyotime, China). The cells were collected by centrifugation, fix with 70% ethanol store at 4°C overnight. The cells were suspended in 500 μL cold PBS with 20 μL RNase A solution at 37°C for 30 minutes. After filtration using

a 400-mesh screen, the cells were resuspended in 400 μL PI and incubated at 4°C in the dark for 30 minutes. Finally, the cells were analyzed by flow cytometry (Beckman Coulter, USA).

2.13 | Luciferase reporter assay

TGF-β2 sequences contain the target sites for miR-149-5p candidates were synthesized and cloned into pSI-Check2 reporter vector downstream to firefly luciferase (pSI-Check2-TGF-β2-wildtype), mutant version of TGF-β2 (pSI-Check2- TGF-β2-mutant) was also generated with the deletion of complementary sites, respectively. The reporter vector, miR-149-5p mimics or negative control werebco-transfected in HEK-293T cells using Lipofectamine 3000 (Invitrogen, CA). Activity of firefly and renilla luciferase were measured by the dual-luciferase system (Promega, USA) according to the manufacturer's protocol and detected by GloMax Multi Jr (Promega, USA).

2.14 | Statistical analysis

Data collected from this study were expressed as mean ± SEM and analyzed using one-way analysis of variance (ANOVA), followed by Newman–Keuls post hoc test (Prism 5.0 GraphPad Software, USA).

3 | RESULTS

3.1 | Upregulation of circUbe2k expression in CCl_4-induced HF

circUbe2k (mmu_circ_0001350) derives from the host gene Ube2k, called circUbe2k in this study. circUbe2k locates on chromosome chr5: 65957227-65985787 (465nt), the genomic structure suggests that circUbe2k consists of 5 exons (exon 2-6) from the Ube2k gene locus (Figure 1A). In order to evaluate whether the mouse model of carbon tetrachloride (CCl_4)-induced HF, we initially send liver tissues isolated from HF model to perform histopathological studies. Liver injury was observed in HF mouse by H) staining (Figure 1B). The collagen area was showed by Sirius red staining, and the activated HSCs were expressed by α-SMA positive area (Figure 1B). Serum level of aspartate aminotransferase (AST) and alanine aminotransferase (ALT) was higher in CCl_4-induced HF mice compared with vehicle mice (Figure 1C). Furthermore, we found that the protein expression of α-SMA, Col1α1 and the mRNA level of α-SMA, Col1α1, TIMP-1, TGF-β1 were markedly increased in liver tissues isolated from isolated from CCl_4-induced HF mice compared with vehicle mice (Figure 1D,E). It is worth nothing that the result of real-time PCR confirmed the relative expression of circUbe2k was higher in CCl_4-induced HF mice than vehicle mice (Figure 1D). These studies have shown that circUbe2k level is increased in HF mouse, suggesting a hypothesis that cirUbe2k may relate to HSCs activation in HF.

3.2 | Inhibition of circUbe2k alleviates CCl_4-induced HF

Next, based on knowing that circUbe2k was increased in HF, we further investigated the effects of circUbe2k on HF mice. Mice were injected with adeno-associated virus (AAV)-siRNA-circUbe2k to knockdown circUbe2k expression in liver, and control group was injected with empty AAV vector. About CCl_4-induced HF mouse, the protein expression level of α-SMA and Col1α1 was significantly decreased following the circUbe2k knockdown (Figure 2A). Moreover, as showed in Figure 2B, the relative expression of circUbe2k and the mRNA levels of fibrogenic genes (α-SMA, Col1α1) were notably attenuated in CCl_4-treated circUbe2k knockdown mouse compared to the AAV-empty mouse (Figure 2B). H&E and Sirius red staining indicated that inhibition of circUbe2k mitigated CCl_4-induced liver injury and fibrosis compared to AAV-empty-treated mouse, and IHC staining results showed liver α-SMA^+ myofibroblasts immune signal were consistently reduced in HF mice following AAV-siRNA-circUbe2k administration (Figure 3A). The α-SMA-positive area quantitative results were shown in Figure 3A. Both levels of ALT and AST in serum were reduced in AAV-siRNA-circUbe2k-treated HF mice compared to the AAV-empty mice (Figure 3B). Taken together, these observations demonstrated that liver injury and expression of fibrogenic markers were significantly alleviated in HF mice with circUbe2k knockdown in vivo.

3.3 | CircUbe2k is upregulated in activated LX-2 cells stimulated by TGF-β1

To further estimate whether circUbe2k (hsa_circ_0069492) expression is related to HSCs activation in HF, we explored the functional effects of circUbe2k on HF in LX-2 cells (human HSC line with the key features of activated HSCs) in vitro. First, western blotting revealed that the protein expression of fibrogenic genes (α-SMA, Col1α1) were enhanced compared to the control group (Figure 4A). Furthermore, the result of real-time PCR shown that the relative expression of circUbe2k and the mRNA level of α-SMA, Col1α1, TIMP-1, TGF-β1 in LX-2 cells stimulated with TGF-β1 (10 ng/mL) (Figure 4B). Consistently, this result indicated that circUbe2k enhanced in LX-2 cells stimulated with TGF-β1, and as the same expression in CCl_4-induced HF mice.

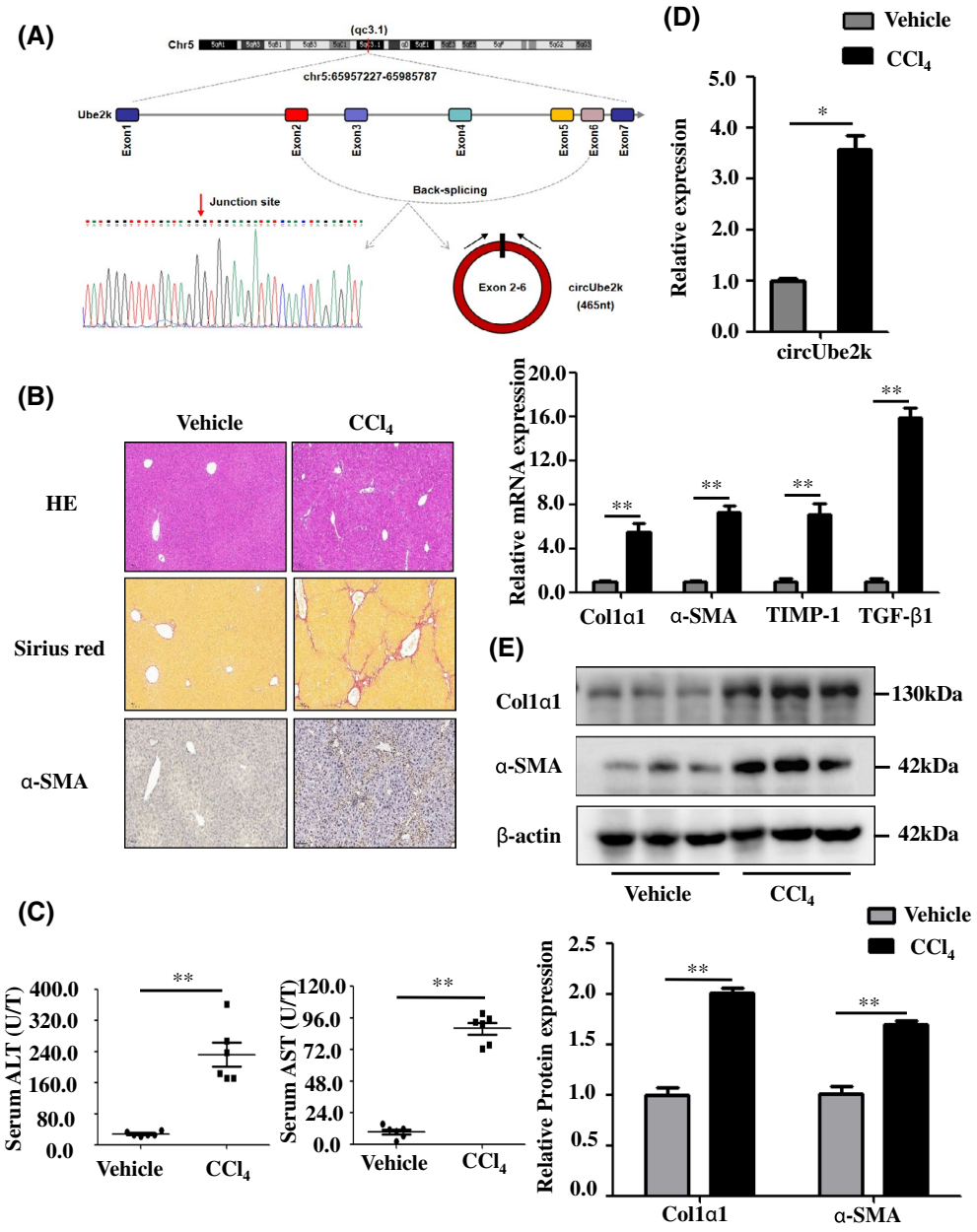

FIGURE 1 Upregulation of circUbe2k in CCl_4-induced hepatic fibrosis. A, Schematic diagram showed the genomic location and back-splicing pattern of circUbe2k. The sanger sequencing of circUbe2k, the arrow represents the "head-to-tail" splicing site. B, Hematoxylin and eosin (H&E), Sirius red staining and immunohistochemistry (IHC) were performed in CCl_4-treated and vehicle mouse. Representative images were shown, scale bar, 100 μM. C, Serum ALT and AST level were determined in CCl_4-treated and vehicle mouse. D, Relative expression of circUbe2k and the fold change of α-SMA, Col1α1, TIMP-1, TGF-β1 mRNA level were shown by real-time PCR in liver tissues from vehicle and CCl_4-treated mouse. E, Relative protein expression of α-SMA and Col1α1 by western blot in liver tissues from vehicle and CCl_4-treated mouse. The data represent the mean ± SEM. For at least three independent experiments. $^*P < .05$, $^{**}P < .01$ vs vehicle group

3.4 | Blocking circUbe2k attenuates LX-2 cells activation and proliferation

Next, to explore the functional role of circUbe2k in LX-2 cells, loss-of-function assays was performed, respectively. First, we constructed a siRNA target to the back-splicing site of circUbe2k and confirmed the silencing efficiency of siRNA-circUbe2k in LX-2 cells after transfection (Figure 5A). Real-time PCR indicated that circUbe2k expression was decreased in activated LX-2 cells with siRNA-circUbe2k transfected (Figure 5B). Moreover, knockdown of circUbe2k subsequently decreased the mRNA levels of α-SMA and Col1α1 in LX-2 cells (Figure 5C), and the same result was shown in western blotting (Figure 5D). CircUbe2k knockdown significantly inhibited LX-2 cells viability by CCK-8 analysis compare to siRNA-NC transfected group (Figure 5E). Functionally, the result of Edu proliferation assay shown that assessment of DNA synthesis

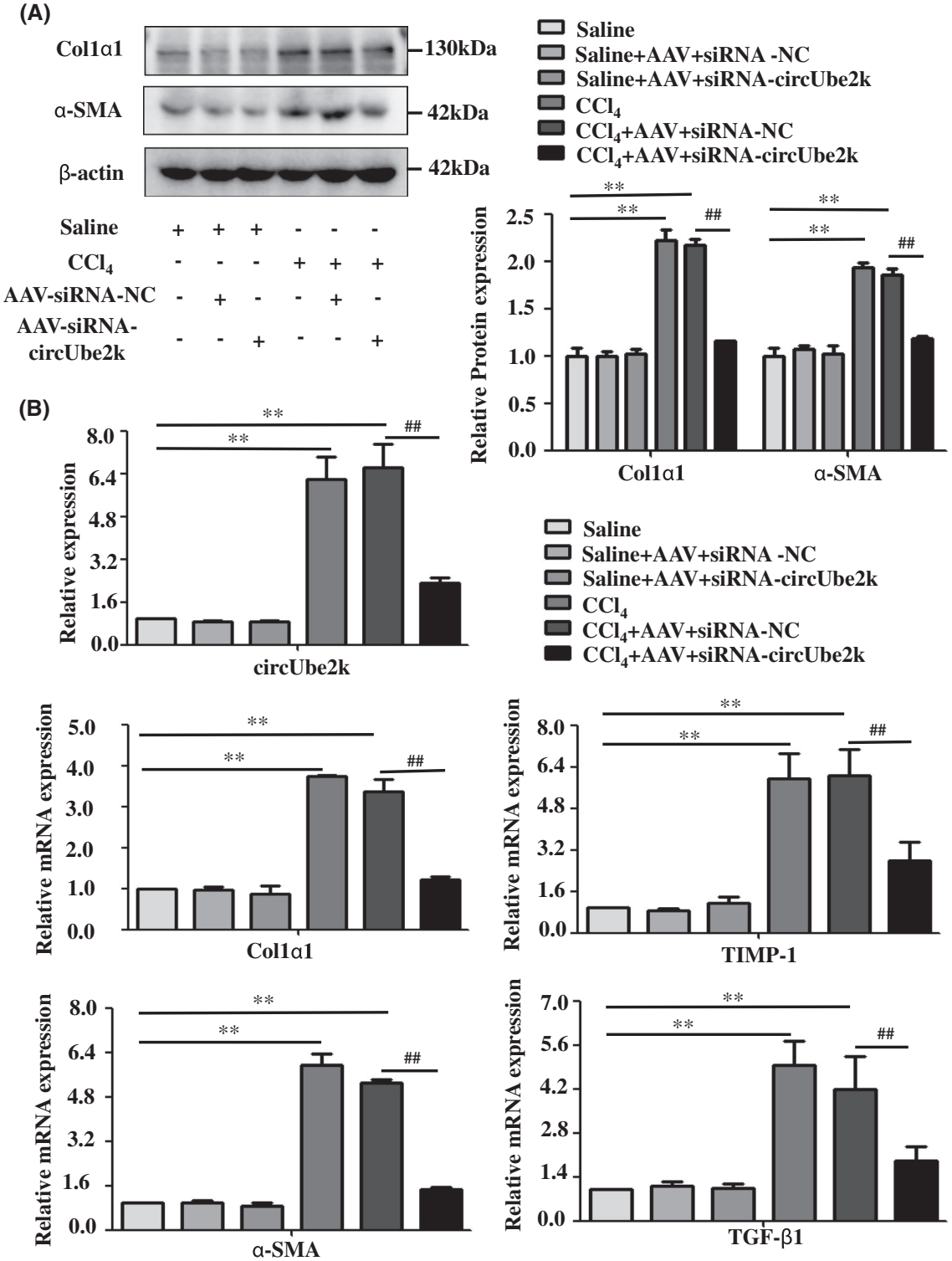

FIGURE 2 Inhibition of circUbe2k alleviates CCl_4-induced hepatic fibrosis. A, Western blot analysis showed the protein expression of α-SMA and Col1α1 decreased with AAV-siRNA-circUbe2k administration. B, Real-time PCR showed relative expression of circUbe2k and the mRNA level of α-SMA, Col1α1 decreased with AAV-siRNA-circUbe2k administration. The data represent the mean ± SEM. For at least three independent experiments. $^{*}P < .05$, $^{**}P < .01$ vs vehicle group; $^{\#}P < .05$, $^{\#\#}P < .01$ vs CCl_4+AAV+siRNA-NC

was obviously decreased in LX-2 cells transfected with siRNA-circUbe2k compared with siRNA-NC (Figure 5F). We further investigated the effect of circUbe2k on the cell cycle of LX-2 cells by Flow cytometry. Inhibition of circUbe2k induced cell cycle arrest in S phase in LX-2 cells stimulated with TGF-β1 (Figure 5G). These results suggest that circUbe2k inhibited the proliferation and activation of HSCs in HF.

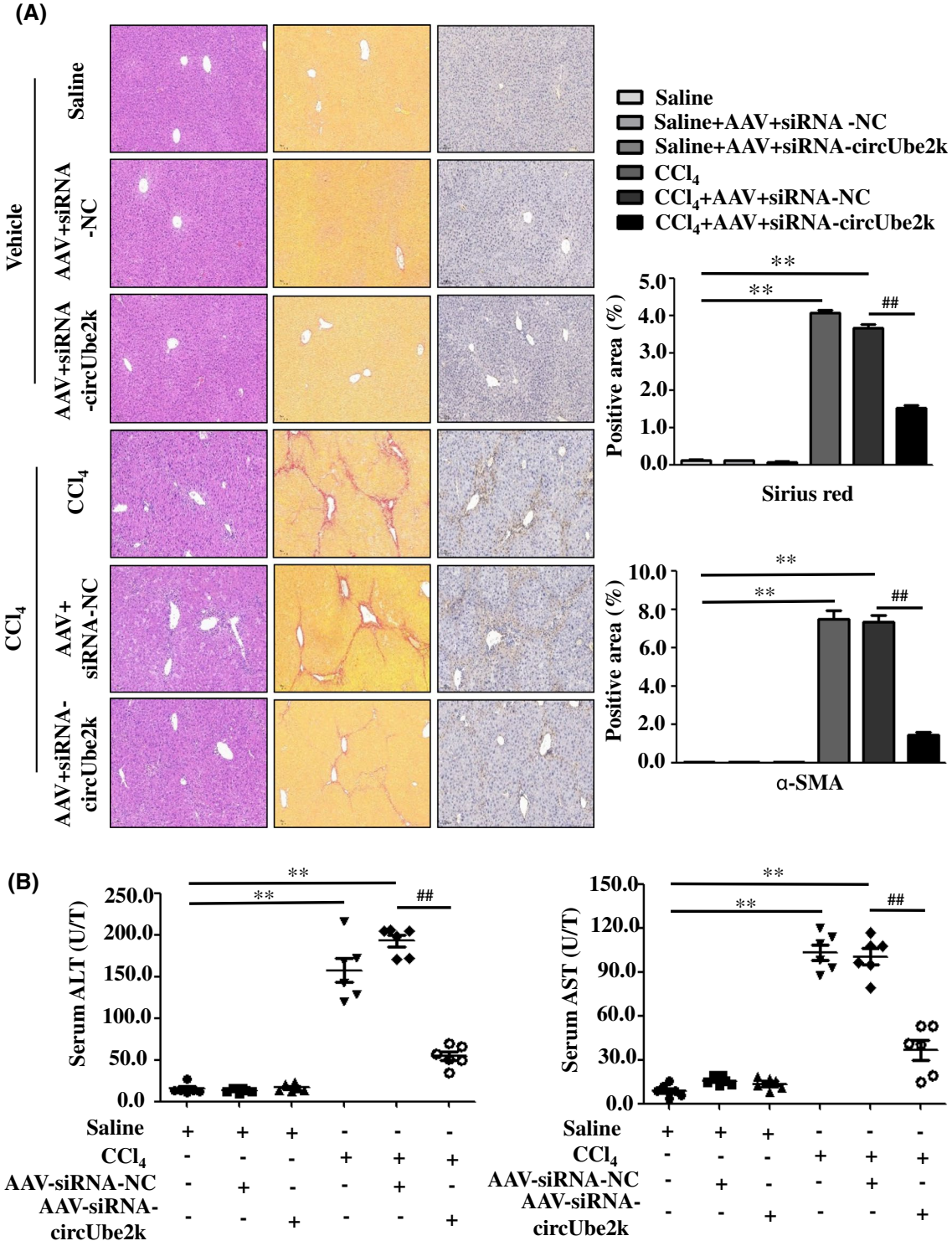

FIGURE 3 Pathology observation of CCl_4-induced hepatic fibrosis with circUbe2k inhibition. A, Pathology observation of H&E staining and Sirius red staining in CCl_4-treated mice following AAV-siRNA-circUbe2k delivery, and IHC of α-SMA. Representative images were presented, scale bar, 100 and 50 μM. Quantification of fibrosis based on immunohistochemistry analysis of α-SMA. B, Serum ALT and AST level were determined in mouse. The data represent the mean ± SEM. For at least three independent experiments. $^{*}P < .05$, $^{**}P < .01$ vs vehicle group; $^{\#}P < .05$, $^{\#\#}P < .01$ vs CCl_4+AAV+siRNA-NC

3.5 | CircUbe2k acts as a competing endogenous RNA interacting with miR-149-5p

Considering the circUbe2k may act as a ceRNA in LX-2 cells. To assess potential miRNAs bind to circUbe2k, and identify promising novel miRNAs relate to HF, miRNA expression in LX-2 cells was analyzed by target prediction tools including TargetScan, circbank, and miRanda. Following the overlapped of prediction result, we found that there were binding sets between circUbe2k and miR-149-5p (Figure 6A). Next,

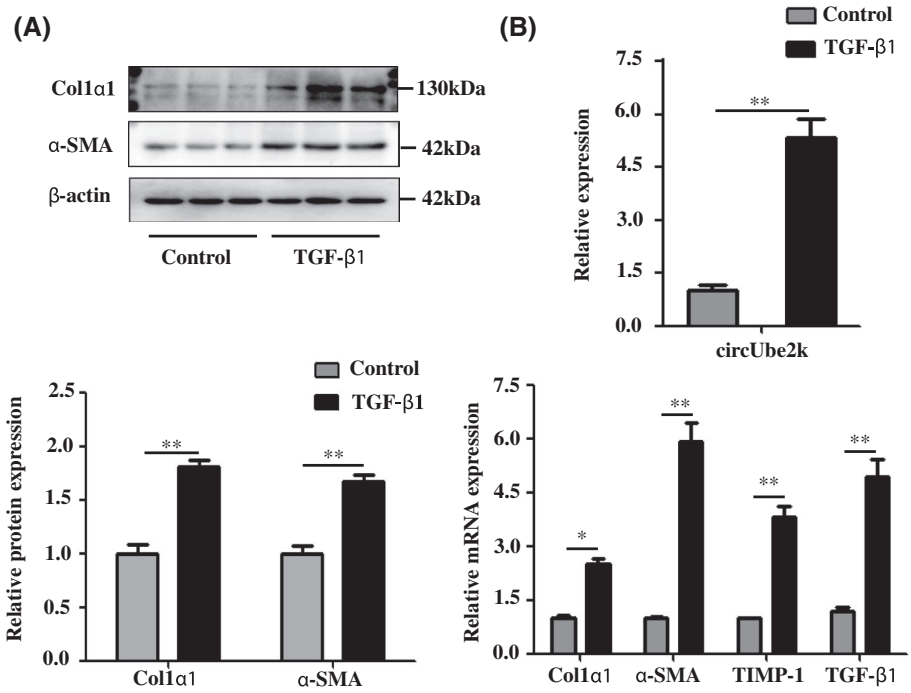

FIGURE 4 CircUbe2k is upregulated in activated LX-2 cells stimulated by TGF-β1. A, Relative protein expression of α-SMA and Col1α1 was measured by western blot in activated LX-2 cells. B, Real-time PCR showed relative expression of circUbe2k and the mRNA level of α-SMA, Col1α1, TIMP-1, TGF-β1 in activated LX-2 cells stimulated by TGF-β1. The data represent the mean ± SEM. For at least three independent experiments. $^{*}P < .05$, $^{**}P < .01$ vs control group

the result of real-time PCR indicated that the relative mRNA expression of miR-149-5p was obviously decreased in CCl_4-induced HF mice, and as the same expression in LX-2 cells stimulated with TGF-β1 (Figure 6B,C). Next, the expression of miR-149-5p was markedly increased in CCl_4-treated circUbe2k knockdown mouse compared to the AAV-empty mouse in vivo (Figure 6D). Interestingly, circUbe2k knockdown also upregulated miR-149-5p level in LX-2 cells following siRNA-circUbe2k administration compared with siRNA-NC (Figure 6E). Therefore, circUbe2k may act as a miR-149-5p sponge to regulate the progression of HF.

3.6 | CircUbe2k upregulates the expression of TGF-β2 by sponging miR-149-5p

To assess potential mRNAs bind to miR-149-5p. mRNA expression in LX-2 cells was analyzed by target prediction tools including TargetScan and miRbase. First, a TGF-β2-3′UTR fragment with wild-type or mutant complementary binding sites was inserted into the luciferase reporter gene pSI-Check2, with miRNA mimics and a negative control were also constructed. Results showed that the Renilla luciferase activity of TGF-β2-3′UTR-wt was significantly inhibited in miR-149-5p mimics groups compared with negative control (Figure 7A). In addition, western blotting indicated that the expression of TGF-β2 was obviously decreased in LX-2 cells following miR-149-5p mimics administration, and on the contrary, the expression of TGF-β2 was increased in LX-2 cells transfected with miR-149-5p inhibitor (Figure 7B). Mechanistically, the result of western blotting shown that TGF-β2 expressions in LX-2 cells were consistently decreased following circUbe2k knockdown. However, the effect of siRNA-circUbe2k treatment on TGF-β2 was further decreased following miR-149-5p level overexpression (Figure 8A). These results demonstrated that circUbe2k acts as a sponge of miR-149-5p to eliminate the effects of miR-149-5p on HF through circUbe2k/miR-149-5p/TGF-β2 axis.

4 | DISCUSSION

circRNAs, a novel class of RNAs with a special structure, was first observed in RNA viruses in the 1970s. Increasing evidence has reported that the involvement of circRNAs in numerous biological processes such as proliferation,[31] metastasis, and therapy resistance. However, the function of majority of identifying circRNAs remains elusive. HF is a significant global concern problem, and there is currently no approved treatment.[28,32] Researches show that HF is a reversible pathological process, which is characteristic by an imbalance between the synthesis and degradation of the

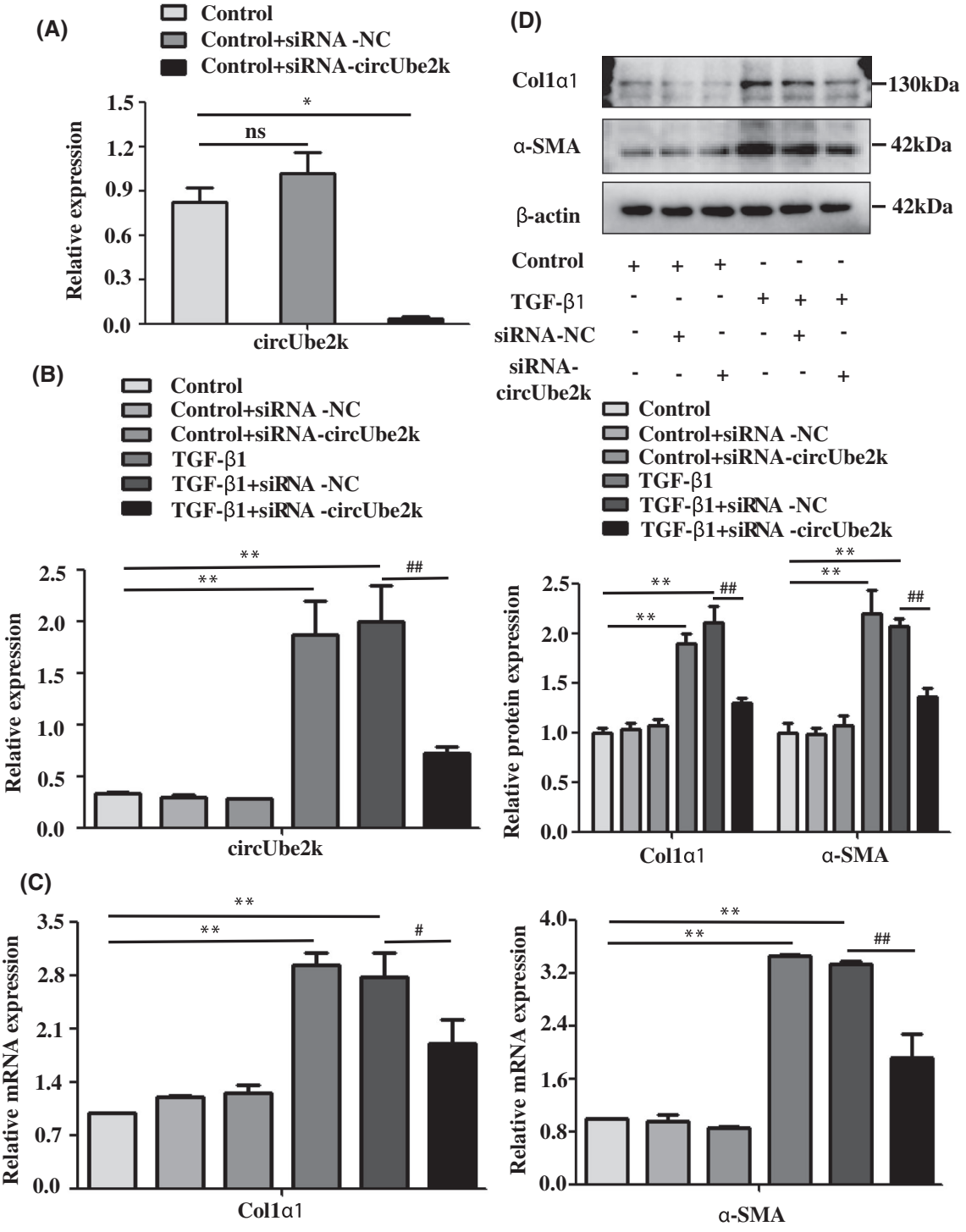

FIGURE 5 Blocking circUbe2k attenuates LX-2 cells activation and proliferation. A, Knockdown efficiency of circUbe2k in LX-2 cells transfected with siRNA- circUbe2k administration. *$P < .05$, **$P < .01$ vs control group. B,C, Real-time PCR showed the relative expression of circUbe2k and the mRNA level of α-SMA, Col1α1 decreased with siRNA-circUbe2k administration. D, Western blot analysis showed the protein expression of α-SMA and Col1α1 decreased with siRNA-circUbe2k administration. E, Relative cells viability measured by CCK8 assay. F, Assessment of DNA synthesis using Edu assay in LX-2 cells, nuclei were stained with Hoechst33342, scale bar, 200 μM. G, Flow cytometry showed the cell cycle distribution in S phase increased following circUbe2k blocking. The data represent the mean ± SEM. For at least three independent experiments. *$P < .05$, **$P < .01$ vs control group; $^{\#}P < .05$, $^{\#\#}P < .01$ vs TGF-β1+siRNA-NC

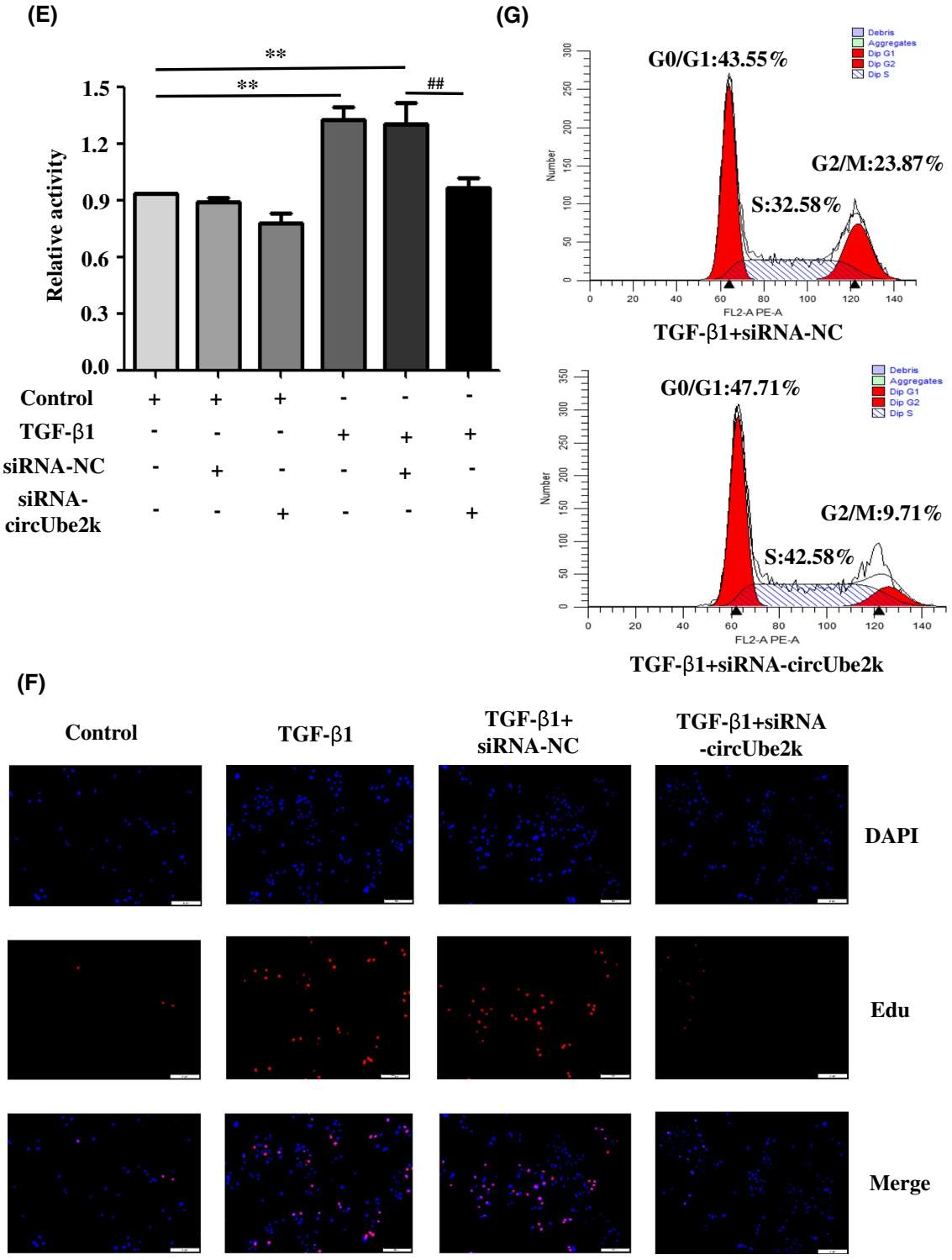

FIGURE 5 (Continued)

ECM leads to abnormal accumulation of fibrous connective tissue in the liver.[33] Interestingly, the activation and proliferation of HSCs caused by liver injury play an important part in the process of HF.[34,35] Increasing evidence has reported the involvement of circRNAs in vital biological processes including HF.[36] Furthermore, circRNAs might be considered as potential biomarkers and therapeutic targets for diseases due to their special stable loop structure.[37,38] However, the molecular mechanisms of circRNAs between HSCs activation and HF formation remain fully unexplored. In our study, we found that the expression of a newly circRNA circUbe2k was increased, which was involved in HF

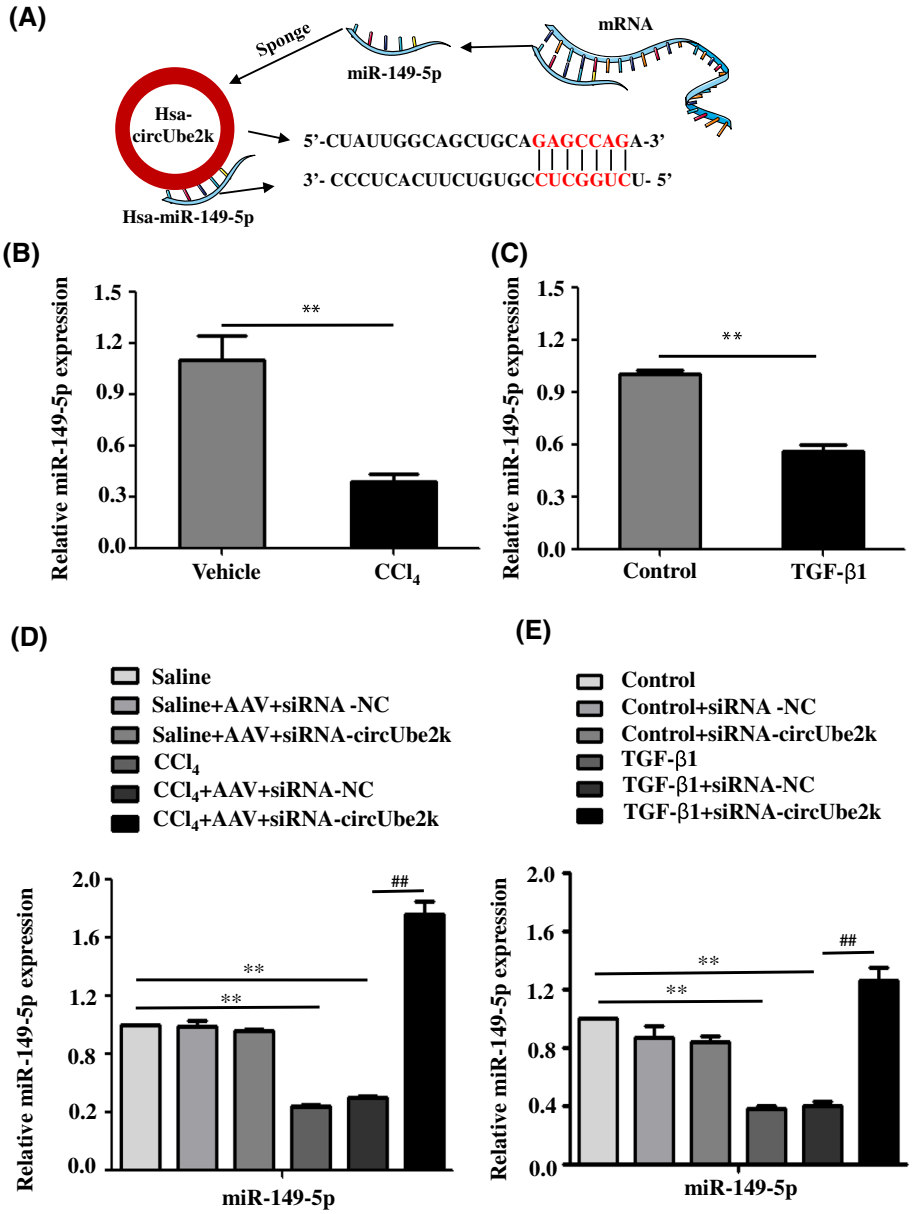

FIGURE 6 CircUbe2k acts as a competing endogenous RNA interacting with miR-149-5p. A, The 3′-UTR of hsa_circ_0069492 harbors miR-149-5p cognate sites. B,C, Relative miR-149-5p expression was measured by real-time PCR in liver tissues from vehicle and CCl_4-treated mouse and activated LX-2 cells stimulated by TGF-β1. D,E, Relative miR-149-5p expression was measured by real-time PCR in liver tissues from AAV-siRNA-circUbe2k administration and activated LX-2 cells transfected with siRNA-circUbe2k administration. The data represent the mean ± SEM. For at least three independent experiments. $^{*}P < .05$, $^{**}P < .01$ vs vehicle group and control group; $^{\#}P < .05$, $^{\#\#}P < .01$ vs CCl_4+AAV-siRNA-NC and TGF-β1+siRNA-NC

and generated reliable data to support the profibrosis effect of circUbe2k. First, we demonstrated the characteristic of circUbes2k, circUbe2k derived from the Ube2k gene. The expression of circUbe2k was in CCl_4-induced HF mice using western blot and real-time PCR showed circUbe2k was upregulated. Furthermore, downregulation of circUbe2k significantly reduced HSCs activation induced the expression of α-SMA, Col1α1, TIMP-1, and TGF-β1. We also discovered that introduction of siRNA-circUbe2k in HSCs inhibited the proliferation and activation of HSCs. In CCl_4-induced HF mice, we found that inhibited the expression of circUbe2k by AAV-siRNA-circUbe2k markedly decreased HF. Our results indicate that circUbe2k may act as a potential therapeutic target for HF.

The study indicated that circRNAs contain multiple miRNA binding sites or miRNA response elements, may act as miRNA sponges.[17] Based on miRNA-mediated mRNA cleavage, circRNAs potentially regulate target gene

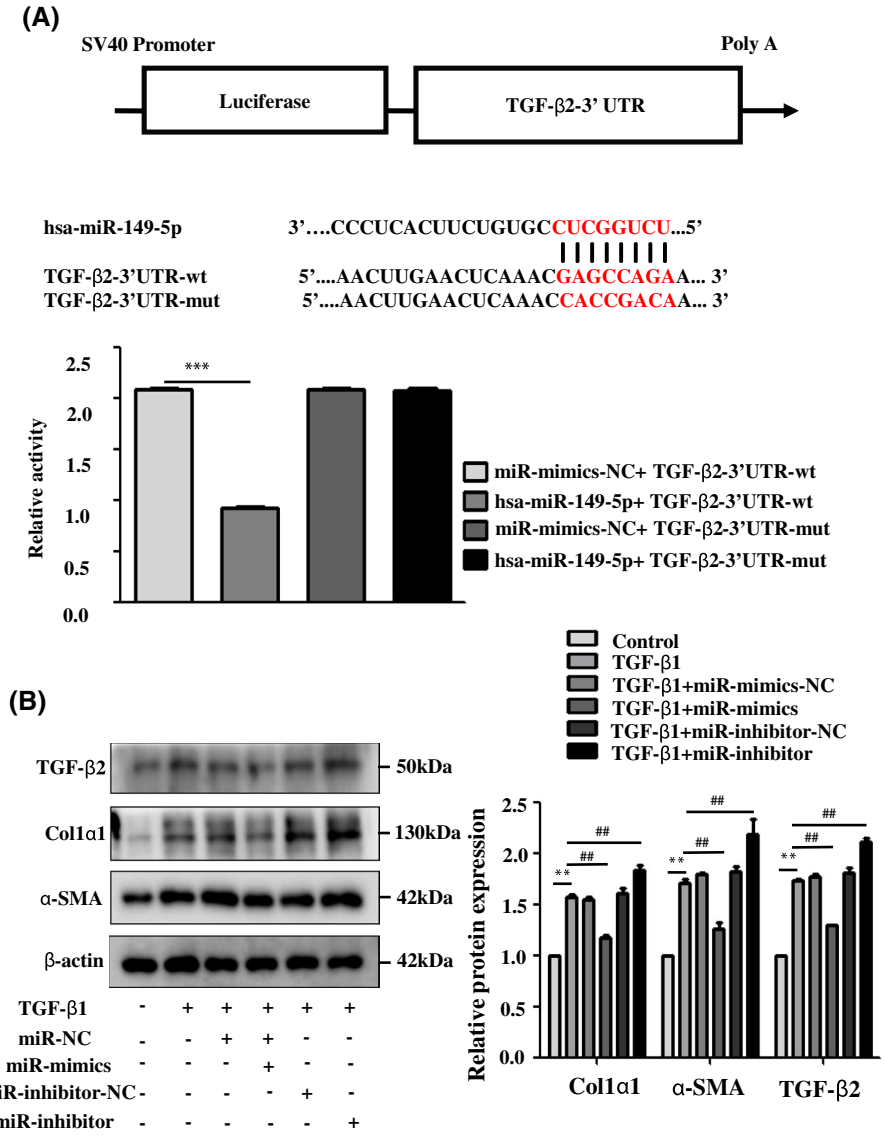

FIGURE 7 miR-149-5p inhibits the expression of TGF-β2. A, The 5′-UTR of miR-149-5p harbors TGF-β2 cognate sites. The renilla luciferase activity analysis of wild type or mutant TGF-β2 and miRNAs mimics or negative control co-transfected into HEK-293T cells, respectively. Data are presented as the ratio of renilla luciferase activity to firefly activity (n = 3). B, Western blot analysis showed the protein expression of TGF-β2 in activated LX-2 cells transfected with miR-149-5p mimics and inhibitor administration. The data represent the mean ±SEM. For at least three independent experiments. $^{*}P < .05$, $^{**}P < .01$ vs control group; $^{\#}P < .05$, $^{\#\#}P < .01$ vs TGF-β1+miR-mimics-NC and TGF-β1+miR-inhibitor-NC

expression. To assess the relationship between circUbe2k and miRNA associated with HF, we selected miRNA that targets circUbe2k by target prediction tools. Mechanistically, circUbe2k function as a modulator by sponging miRNAs. Interestingly, we confirmed that miR-149-5p decreased in HSCs during hepatic fibrogenesis and the expression pattern of miR-149-5p was opposite to circUbe2k. Moreover, we demonstrated that circUbe2k downregulation increased miR-149-5p levels in HSCs. Furthermore, we also revealed that miR-149-5p binds to the 3′UTR of TGF-β2, the expression of TGF-β2 was decreased in liver fibrogenesis following circUbe2k downregulation.

Ultimately, this study indicated a newly regulatory axis formed through circUbe2k/miR-149-5p/TGF-β2 in HF (Figure 9). We explored the way of expression, the function and the mechanism of circUbe2k in HF. However, involvement of circUbe2k in ceRNA mechanisms still needs to be exploring. Our present study indicated that circUbe2k provides a possible future to find an attractive novel decoration for HF.

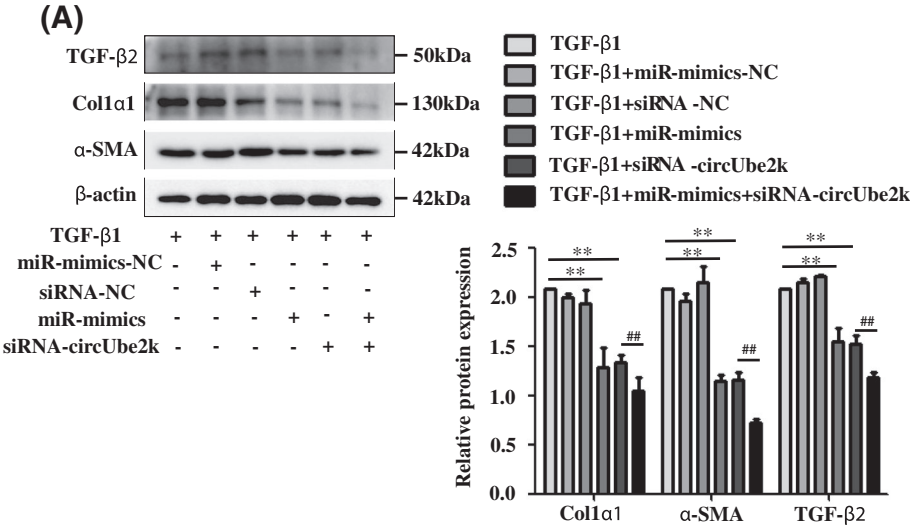

FIGURE 8 CircUbe2k upregulates the expression of TGF-β2 by sponging miR-149-5p. A, Western blot analysis showed the protein expression of TGF-β2 in activated LX-2 cells transfected with siRNA-circUbe2k, miR-149-5p mimics. The data represent the mean ±SEM. For at least three independent experiments. $^{*}P < .05$, $^{**}P < .01$ vs TGF-β1; $^{\#}P < .05$, $^{\#\#}P < .01$ v TGF-β1+siRNA-circUbe2k

FIGURE 9 Circular RNA circUbe2k promotes hepatic fibrosis via sponging miR-149-5p/TGF-β2 axis

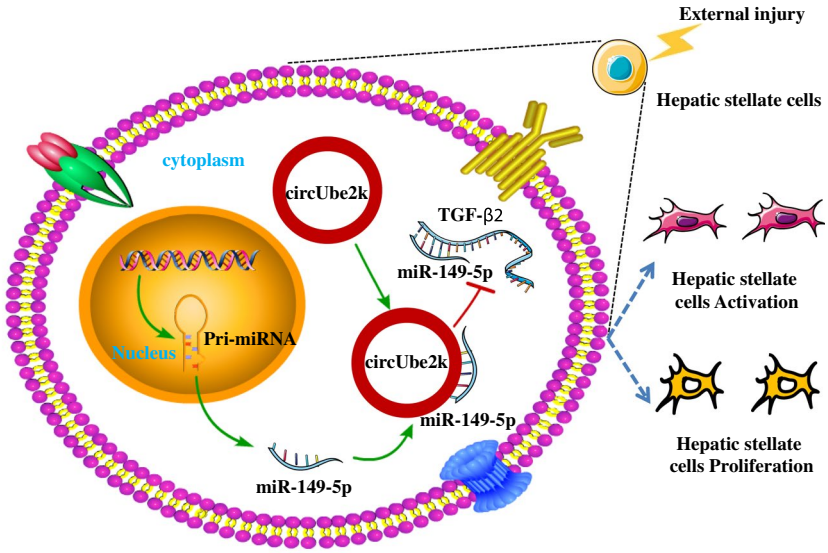

ACKNOWLEDGMENTS

This work was supported by the National Science Foundation of China (Nos. 81770609, 81970534, U19A2001) and Anhui Medical University of Science and Technology (No. 1704a0802161).

DISCLOSURES

The authors declare that they have no competing interests.

AUTHOR CONTRIBUTIONS

J. Li conceived this research; S. Zhu, X. Chen, and J.-N. Wang collected, analyzed, and disposed data; J.-J. Xu, J.-J. Li, A. Wang, S. Wu, Y.-Y. Wu, and X.-F. Li analyzed the tables and assembled the figure; J. Li and C. Huang contributed to all aspects of this study, and revised the manuscript for publication.

REFERENCES

1. Bataller R, Brenner DA. Liver fibrosis. *J Clin Invest*. 2005;115(2):209-218.
2. Gong Y, Yang Y. Activation of Nrf2/AREs-mediated antioxidant signalling, and suppression of profibrotic TGF-beta1/Smad3 pathway: a promising therapeutic strategy for hepatic fibrosis—a review. *Life Sci*. 2020;256:117909.
3. Friedman SL. Molecular regulation of hepatic fibrosis, an integrated cellular response to tissue injury. *J Biol Chem*. 2000;275(4):2247-2250.
4. Zou GL, Zuo S, Lu S, et al. Bone morphogenetic protein-7 represses hepatic stellate cell activation and liver fibrosis via regulation

of TGF-beta/Smad signaling pathway. *World J Gastroenterol*. 2019;25(30):4222-4234.
5. Parola M, Pinzani M. Liver fibrosis: pathophysiology, pathogenetic targets and clinical issues. *Mol Aspects Med*. 2019;65:37-55.
6. Tan S, Lu Y, Xu M, et al. beta-Arrestin1 enhances liver fibrosis through autophagy-mediated Snail signaling. *FASEB J*. 2019;33(2):2000-2016.
7. Zhou L, Shi M, Zhao L, et al. Clonorchis sinensis lysophospholipase A upregulates IL-25 expression in macrophages as a potential pathway to liver fibrosis. *Parasit Vectors*. 2017;10(1):295.
8. Yu HX, Yao Y, Bu FT, et al. Blockade of YAP alleviates hepatic fibrosis through accelerating apoptosis and reversion of activated hepatic stellate cells. *Mol Immunol*. 2019;107:29-40.
9. Cherubini A, Barilani M, Rossi RL, et al. FOXP1 circular RNA sustains mesenchymal stem cell identity via microRNA inhibition. *Nucleic Acids Res*. 2019;47(10):5325-5340.
10. Pandey PR, Yang JH, Tsitsipatis D, et al. circSamd4 represses myogenic transcriptional activity of PUR proteins. *Nucleic Acids Res*. 2020;48(7):3789-3805.
11. Nigro JM, Cho KR, Fearon ER, et al. Scrambled exons. *Cell*. 1991;64(3):607-613.
12. Capel B, Swain A, Nicolis S, et al. Circular transcripts of the testis-determining gene Sry in adult mouse testis. *Cell*. 1993;73(5):1019-1030.
13. Yu R, Yao J, Ren Y A novel circRNA, circNUP98, a potential biomarker, acted as an oncogene via the miR-567/ PRDX3 axis in renal cell carcinoma. *J Cell Mol Med*. 2020;24(17):10177-10188. http://dx.doi.org/10.1111/jcmm.15629
14. Li H, Shan C, Wang J. CircRNA Hsa_circ_0001017 inhibited gastric cancer progression via acting as a sponge of miR-197. *Dig Dis Sci*. 2020. http://dx.doi.org/10.1007/s10620-020-06516-8
15. Li X, Ma N, Zhang Y, et al. Circular RNA circNRIP1 promotes migration and invasion in cervical cancer by sponging miR-629-3p and regulating the PTP4A1/ERK1/2 pathway. *Cell Death Dis*. 2020;11(5):399.
16. Jeck WR, Sharpless NE. Detecting and characterizing circular RNAs. *Nat Biotechnol*. 2014;32(5):453-461.
17. Shi Y, Fang N, Li Y. Circular RNA LPAR3 sponges microRNA-198 to facilitate esophageal cancer migration, invasion, and metastasis. *Cancer Sci*. 2020;111(8):2824-2836. http://dx.doi.org/10.1111/cas.14511
18. Du WW, Yang W, Liu E, Yang Z, Dhaliwal P, Yang BB. Foxo3 circular RNA retards cell cycle progression via forming ternary complexes with p21 and CDK2. *Nucleic Acids Res*. 2016;44(6):2846-2858.
19. Chen H, Liu Y, Li P, Zhu D. RE: novel role of FBXW7 circular RNA in repressing glioma tumorigenesis. *J Natl Cancer Inst*. 2019;111(4):435.
20. Yang Y, Gao X, Zhang M, et al. Novel role of FBXW7 circular RNA in repressing glioma tumorigenesis. *J Natl Cancer Inst*. 2018;110(3):304-315.
21. Xu G, Li M, Wu J, Qin C, Tao Y, He H. Circular RNA circNRIP1 sponges microRNA-138-5p to maintain hypoxia-induced resistance to 5-Fluorouracil through HIF-1alpha-dependent glucose metabolism in gastric carcinoma. *Cancer Manag Res*. 2020;12:2789-2802.
22. Luo Z, Rong Z, Zhang J, et al. Circular RNA circCCDC9 acts as a miR-6792-3p sponge to suppress the progression of gastric cancer through regulating CAV1 expression. *Mol Cancer*. 2020;19(1):86.
23. Zhu S, Chen X, Chen Y. Role of microRNAs in hepatic stellate cells and hepatic fibrosis: an update. *Curr Pharm Des*. 2020;26. http://dx.doi.org/10.2174/1381612826666201023143542
24. He Y, Feng D, Li M, et al. Hepatic mitochondrial DNA/Toll-like receptor 9/MicroRNA-223 forms a negative feedback loop to limit neutrophil overactivation and acetaminophen hepatotoxicity in mice. *Hepatology*. 2017;66(1):220-234.
25. Yang JJ, Tao H, Liu LP, Hu W, Deng ZY, Li J. miR-200a controls hepatic stellate cell activation and fibrosis via SIRT1/Notch1 signal pathway. *Inflamm Res*. 2017;66(4):341-352.
26. Chen X, Li HD, Bu FT, et al. Circular RNA circFBXW4 suppresses hepatic fibrosis via targeting the miR-18b-3p/FBXW7 axis. *Theranostics*. 2020;10(11):4851-4870.
27. Chen X, Li XF, Chen Y, et al. Hesperetin derivative attenuates CCl4-induced hepatic fibrosis and inflammation by Gli-1-dependent mechanisms. *Int Immunopharmacol*. 2019;76:105838.
28. Chen Y, Chen X, Ji YR, et al. PLK1 regulates hepatic stellate cell activation and liver fibrosis through Wnt/beta-catenin signalling pathway. *J Cell Mol Med*. 2020;24(13):7405-7416.
29. Chen YH, Yuan BY, Wu ZF, Dong YY, Zhang L, Zeng ZC. Microarray profiling of circular RNAs and the potential regulatory role of hsa_circ_0071410 in the activated human hepatic stellate cell induced by irradiation. *Gene*. 2017;629:35-42.
30. Lan HY, Hutchinson P, Tesch GH, Mu W, Atkins RC. A novel method of microwave treatment for detection of cytoplasmic and nuclear antigens by flow cytometry. *J Immunol Methods*. 1996;190(1):1-10.
31. Cedric BC, Souraka TDM, Feng YL, Kisembo P, Tu JC. CircRNA ZFR stimulates the proliferation of hepatocellular carcinoma through upregulating MAP2K1. *Eur Rev Med Pharmacol Sci*. 2020;24(19):9924-9931.
32. Pinheiro D, Dias I, Ribeiro Silva K, et al. Mechanisms underlying cell therapy in liver fibrosis: an overview. *Cells*. 2019;8(11):1339.
33. Huang YH, Chen MH, Guo QL, Chen ZX, Chen QD, Wang XZ. Interleukin-10 induces senescence of activated hepatic stellate cells via STAT3-p53 pathway to attenuate liver fibrosis. *Cell Signal*. 2020;66:109445.
34. Yan J, Huang H, Liu Z, et al. Hedgehog signaling pathway regulates hexavalent chromium-induced liver fibrosis by activation of hepatic stellate cells. *Toxicol Lett*. 2020;320:1-8.
35. Friedman SL. Mechanisms of hepatic fibrogenesis. *Gastroenterology*. 2008;134(6):1655-1669.
36. Jin H, Li C, Dong P, Huang J, Yu J, Zheng J. Circular RNA cMTO1 promotes PTEN expression through sponging miR-181b-5p in liver fibrosis. *Front Cell Dev Biol*. 2020;8:714.
37. Zhang Z, Xie Q, He D, et al. Circular RNA: new star, new hope in cancer. *BMC Cancer*. 2018;18(1):834.
38. Meng S, Zhou H, Feng Z, et al. CircRNA: functions and properties of a novel potential biomarker for cancer. *Mol Cancer*. 2017;16(1):94.

SUPPORTING INFORMATION

Additional supporting information may be found online in the Supporting Information section.

How to cite this article: Zhu S, Chen X, Wang J-N, et al. Circular RNA circUbe2k promotes hepatic fibrosis via sponging miR-149-5p/TGF-β2 axis. *The FASEB Journal*. 2021;35:e21622. https://doi.org/10.1096/fj.202002738R